Tectonophysics xxx (2015) xxx–xxx

Contents lists available at ScienceDirect

Tectonophysics

journal homepage: www.elsevier.com/locate/tecto

The September 27, 2012, M_L 4.1, Benevento earthquake: A case of strike-slip faulting in Southern Apennines (Italy)

Guido Maria Adinolfi [a,*], Raffaella De Matteis [b], Antonella Orefice [c], Gaetano Festa [c], Aldo Zollo [c], Rita de Nardis [a,d], Giusy Lavecchia [a]

[a] GeosisLab, DiSPUTer, Università "G. d'Annunzio", Campus Universitario, Chieti Scalo, CH, Italy
[b] Dipartimento di Scienze e Tecnologie, Università degli Studi del Sannio, Benevento, Italy
[c] RISSC-Lab, Dipartimento di Fisica, Università di Napoli Federico II, Naples, Italy
[d] Dipartimento della Protezione Civile, Via Vitorchiano, 4, 00189 Rome, Italy

ARTICLE INFO

Article history:
Received 15 September 2014
Received in revised form 2 June 2015
Accepted 25 June 2015
Available online xxxx

Keywords:
Study of background seismicity
Earthquake re-location
Seismotectonics
Southern Apennines (Italy)
Strike-slip faulting
Benevento earthquake

ABSTRACT

On September 27, 2012 at 01:08 (UTC) a M_L 4.1 earthquake started a seismic sequence approximately 10 km east of the city of Benevento, in Southern Apennines (Italy). During the following four days, about 40 events with M_L ranging between 1.3 and 4.1 were detected in the same area, where the seismic hazard is one of the largest of the Italian Peninsula and where several historical and destructive events took place. In order to investigate the seismicity spatio-temporal pattern and to identify the seismogenic source geometry, a detailed analysis was performed integrating data recorded at three different seismic networks. The earthquakes were relocated using the double-difference technique and focal mechanism solutions were obtained by the moment tensor inversion. Also, to better understand the rupture process, seismic source parameters were estimated and apparent source time functions were inverted to retrieve the slip distribution for the largest magnitude event. Our results show the existence in the study area of roughly E–W striking fault plane with a right-lateral strike-slip kinematics, seated at mid-crustal depths (10–20 km), revealing a characteristic seismicity quite different from that typically associated to the outcropping NW–SE-striking active normal faults that are responsible of moderate to large earthquakes in the Southern Apennines axial sector.

In this work, we address questions concerning i) the presence in the Benevento area of a mid-crust seismogenic strike-slip fault, previously unrecognized; ii) its link to the regional seismotectonic setting; and iii) the existence of a strike-slip tectonic regime that uniformly extends in the footwall of the Apennines thrust at relevant depth, not only in the Apulian foreland, as demonstrated to date, but also under the mountain chain axial zone.

1. Introduction

During three days between September 27 and 30, 2012 about 40 earthquakes occurred nearby Benevento (Fig. 1a), a town located in one of the most seismic active areas of Southern Apennines (Italy) and whose city center is rich of historical buildings. The seismic sequence was characterized by low energy with the largest magnitude events concentrated on September 27 at 01:08 (M_L 4.1), 03:47 (M_L 3.5), and 08:35 (M_L 3.7), all times being in UTC. During its long history, Benevento was struck by several earthquakes that produced numerous causalities and severe damage (Fig. 1b). The most destructive event (Io = XI; M_w = 7.2; Rovida et al., 2011) occurred in 1456, with more than 30,000 causalities and an associated MCS intensity (Is) of IX over an area of 20,000 km^2 in Southern Italy (Iannaccone et al., 1995). Afterwards, different earthquakes with Io = X–XI, as described later on, hit the Benevento province (Rovida et al., 2011). In the last decades, the seismicity of the Sannio area has occurred as low energy swarms and sparse events (M < 3.7; Milano et al., 2006). For this reason, considering the recurrence time of large historical earthquakes, this region shows one of the highest seismogenic potentials of the Italian country (Chiarabba and Amato, 1997; Improta et al., 2000).

Low energy swarms and sparse events (e.g. micro-seismicity) can improve the seismotectonic knowledge of an area. Several worldwide studies define the fine scale fault geometry tracking the background seismicity pattern through an accurate earthquake location (De Matteis et al., 2012; Hauksson and Shearer, 2005; Lin et al., 2007; Romano et al., 2013a,b; Rubin et al., 1999; Stabile et al., 2012; Waldhauser and Ellsworth, 2000). The analysis of the micro-seismicity represents a peculiar tool to get specific information about active faults and to study the associated spatio-temporal seismicity even if some limitations are due to the absence of dense local networks, number and quality of the data, large hypocentral errors and inaccuracy of the crustal

* Corresponding author.
E-mail address: g.adinolfi@unich.it (G.M. Adinolfi).

http://dx.doi.org/10.1016/j.tecto.2015.06.036

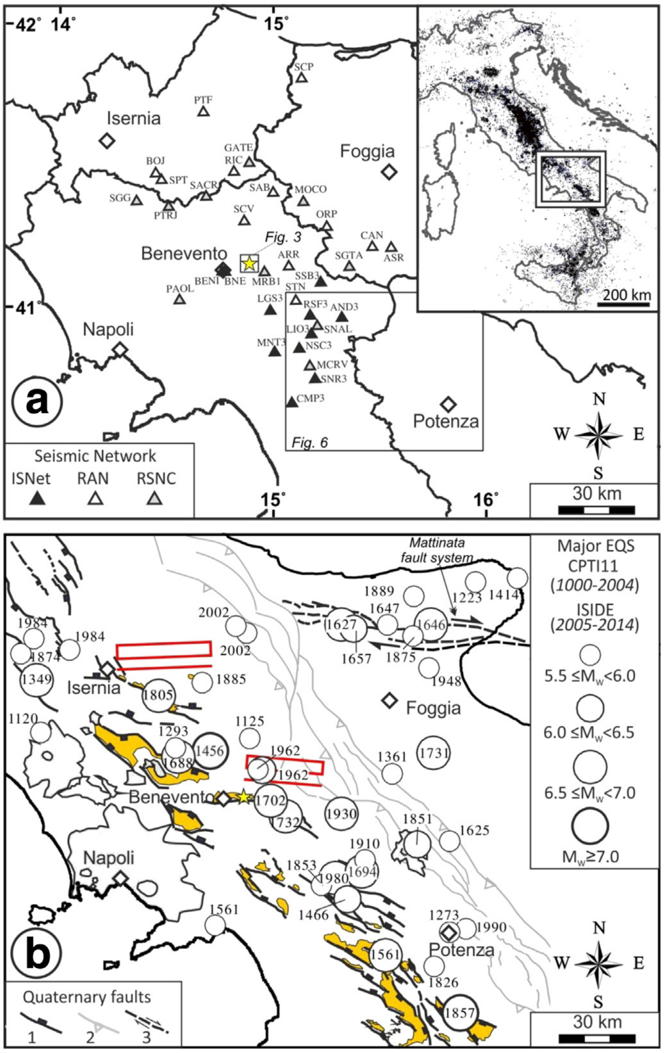

Fig. 1. a) Map showing the mainshock of 2012 Benevento seismic sequence (September 27 at 01:08, M_L 4.1; star symbol) and the seismic stations used in the data analysis. Key: ISNet — Irpinia Seismic Network (Weber et al., 2007); RAN — Italian strong motion network (Gorini et al., 2010; Zambonelli et al., 2011); RSNC — Centralized National Seismic Network. Benevento area of Fig. 3 and Irpinia — ISNet study area of Fig. 6 are indicated. In the location map, Italian instrumental seismicity from 2005 to 2103 is displayed (Italian Seismological Instrumental and Parametric Data-Base, ISIDE). b) Active faults in Southern Italy (after Brozzetti, 2011) with major historical and instrumental earthquakes from current catalogues (Parametric Catalogue of Italian Earthquakes, CPTI11, Rovida et al., 2011; Italian Seismicity Catalogue, CSI, Castello et al., 2006; ISIDE). The earthquakes highlighted with gray circles are discussed in the text. Seismogenic (box-shaped) sources of the 1456 earthquake as proposed by Fracassi and Valensise (2007) are displayed as the fault projections to the ground surface. Key: 1, normal faults; 2, thrust faults; 3, strike-slip faults.

velocity model. However, this analysis has a particular relevance in areas characterized by geological complexities or by seismogenic structures seated at large depths where the crustal structure and fault pattern are inaccurate or indefinite.

In this work, we performed a detailed analysis of the 2012 Benevento seismic sequence integrating data recorded at 31 seismic stations of different networks. After a manual picking of the P- and S-wave arrival times, we relocated the earthquakes using the double-difference technique to minimize errors related to uncertainty in the 3-D crustal velocity model. In addition, we carried out a complete rupture analysis: after computing the focal mechanisms, we estimated the apparent source time functions and we mapped it onto the fault plane to define the slip distribution for the largest event in the sequence. We computed the source parameters for the two largest earthquakes to deeply investigate the rupture mechanism from the estimates of the seismic moment M_0 and the source radius.

2. Tectonic setting

The Benevento earthquake epicentral area is located in the axial sector of the late Miocene–Pliocene Southern Apennines fold-and-thrust belt, dissected by later Quaternary extensional structures (Brozzetti, 2011 and references therein).

The present structural–geological setting of the study area is extremely complex due to the variety of the paleogeographic domains involved in mountain chain building (Cavazza et al., 2004; Mostardini and Merlini, 1986; Nicolai and Gambini, 2007; Patacca and Scandone, 2007; Vezzani et al., 2010).

From west to east, they include: i) the pelagic domain formerly located in between the Alpine Tethys and the Adriatic foreland (e.g. the middle Jurassic–early Miocene Sicilide units); ii) the Apennine carbonate platform units (e.g. late Trias–middle Miocene), originally corresponding to the western edge of the Adria plate; iii) the Lagonegro and Sannio–Molise pelagic units (middle Triassic–early Cretacic pelagites and Burdigalian–Messinian flysch deposits) and iv) to the Apulian outer carbonate platform (e.g. a thick succession, up to 6000 m, of shallow water carbonates and anhydrites, of late Triassic–late Miocene age) deposited on the eastern side of Adria (Supplementary Fig. S1).

The geometric setting is further complicated by 1) the abundance of syn-orogenic Tertiary deposits progressively involved in the eastward-migrating compressional deformation, 2) the non-cylindrical configuration of the propagating compression, also associated to strike-slip deformation zones that cause bending of the structural trends, 3) the local presence of back-thrust and out-of-sequence thrust, and 4) the final dissection of the overall thrust belt by extensional structures.

The structural style of the inner compressional belt of Southern Italy, which mainly involves the Apennine carbonate platform and the Lagonegrese units, is largely interpreted as thin-skinned and characterized by duplex geometries and out-of-sequence thrusts (Cavazza et al., 2004; Mostardini and Merlini, 1986), but conflicting interpretations are proposed in the literature on the provenance of the various units. In particular, the Lagonegrese and Sannio–Molise units were mostly interpreted as a complex stack of rootless sheets, sandwiched in between the Apennine and Apulian Platforms (Mostardini and Merlini, 1986; Vezzani et al., 2010), an alternative view, proposed by Patacca and Scandone (2007) refers to the Sannio sheet, associated to the southern margin of the Tethys Ocean (west of the Apennine Platform), and attributes it to a higher structural position. Alternative interpretations concern also the crustal-scale tectonic style of thrusting, that is assumed as thin-skinned by most authors (Cavazza et al., 2004; Mostardini and Merlini, 1986; Patacca and Scandone, 2007; Scrocca et al., 2005, 2007; Vezzani et al., 2010) and as thick-skinned by a few others (Menardi Noguera and Rea, 2000).

Conversely, the structural style of the outer compressional belt, which mainly involves the Apulian Platform carbonates, is often interpreted as typically thick-skinned (Butler et al., 2000; Menardi Noguera and Rea, 2000; Shiner et al., 2004), with thrust faults penetrating across the basement and possibly reaching the base of the crust.

Starting from early–middle Pleistocene times (Brozzetti, 2011; Cinque et al., 1993), the axial portion of the chain had undergone a marked uplift during which the activity of NW–SE striking normal fault alignments, that locally follow arcuate trends often parallel to previous frontal thrusts, was coupled with thermal/isostatic regional raising. Several narrow and asymmetrical intramontane basins originated by block faulting and were filled by syn-tectonic continental deposits. Field data and seismic profile interpretation show that these basins are bounded by high-angle SSW- to WSW-dipping normal and normal-oblique faults and by E-dipping faults. The latter show at depths that a low-angle geometry plays the role of basal detachments (Brozzetti, 2011). The overall extensional belt extends with continuity along the axial zone of the Southern Apennines and is associated to a relevant historical and instrumental seismic activity (maximum magnitudes M = 7) (Basili et al., 2008; Chiarabba et al., 2005; Rovida et al., 2011).

The undeformed Apulian Plio-Pleistocene foreland, at the footwall of the outer thrust front, is dissected by normal and strike-slip faults, trending from NW–SE to E–W and ranging in age from Mesozoic to Pleistocene (Pieri et al., 1997). An E–W strike-slip fault zone, with left lateral kinematics in Pliocene times and right-lateral kinematics in Quaternary times is well exposed in the Gargano promontory and is known as Mattinata fault zone (Billi, 2003; Tondi et al., 2005). The Mattinata fault continues eastward in the offshore Gondola strike-slip system and westward in the buried Molise strike-slip structure that originated the 31 October and 1 November 2002, M_w 5.7, Molise earthquakes (Di Bucci et al., 2010).

3. Historical and instrumental seismicity

Several large historical destructive earthquakes hit the Southern Apennines causing severe damage and many fatalities. Devastating effects in the Benevento province, with intensity up to X–XI MCS, were produced by the 1456, 1688, 1694, 1702, 1732, 1805, and 1930 earthquakes (gray symbols in Fig. 1b). The macroseimic epicenter of several events with Io ≥ VI (1019, 1044, 1094, 1139, 1702) was just located close to the town of Benevento (Rovida et al., 2011), which was also struck by a number of moderate seismic swarms that occurred on 1885, 1903 and 1905 (Alessio et al., 1996).

Most of the significant earthquakes in Southern Italy, such as the 1962 (M_L 6.1) and the Irpinia 1980 earthquake (M_S 6.9), occurred along the intra-Apennines extensional belt, activating predominately eastward-dipping, normal and normal-to-oblique individual sources (Basili et al., 2008; DISS Working Group, 2010; Valensise and Pantosti, 2001). In detail, the August 21, 1962 earthquake sequence involved a series of small foreshocks followed by a large one with M_L 5.7 at 18:09, a mainshock with M_L 6.1 at 18:19 and many aftershocks including the one at 18:44 with M_L 6.0. Westaway and Jackson (1987) also re-located the main events of the sequence relative to the November 23, 1980 (M_S 6.9) event, using the data recorded at the same stations that were operating in the 1980. Their results show that the depth of these events is about 8 km and occurred on steep normal faults striking NW–SE and dipping NE, that bounded an intra-Apennines sedimentary basin situated at NE in the hanging wall of the fault, similar to the structural geological setting deduced for the 1980 earthquake (Westaway and Jackson, 1987).

Conversely, the large 1456 earthquake (Io XI; M_w 7.2), which consisted of a multiple earthquake sequence with three main major events, has been attributed by Fracassi and Valensise (2007) to the activation of distinct east–west oblique right-lateral strike-slip structures across the Apulian foreland. The earliest mainshock (5 Dec 1456, M_w 7.0; DISS Working Group, 2010) occurred in the Sannio region, in the Ariano Irpino–Paduli mesoseismal area, where a seismogenic source, not far from the Benevento town, is located between the external part of the thrust belt and the Apulian foreland (DISS Working Group, 2010) (Fig. 1b).

The recent seismicity in the Sannio–Matese has been monitored since 1980 (Milano et al., 2006), when the areal coverage of the Centralized National Seismic Network (RSNC) was reasonably sufficient to get more accurate information as compared to the past. Nevertheless, the location and focal mechanism determinations were possible only for 1990–1992 low magnitude events (M_L ≤ 3.7), thanks to the integration of local and temporary seismic networks (Alessio et al., 1996; Federici et al., 1992). Present background seismicity consists of sparse isolated earthquakes with M_d < 3 and depths within the first 20 km (Milano et al., 2002) (Supplementary Fig. S2).

The 1990 seismic sequence occurred between April and July 1990 north of Benevento with a local magnitude ranging between 1.0 and 3.6 (Alessio et al., 1996). It was composed by events homogenously distributed within the first 15 km, showing no particular alignment and different types of faulting motions coherently with the regional strain field (T axes with NE–SW orientation). The following seismicity was characterized by two seismic swarms that occurred in June 1991 and in March 1992, concentrated north and north-east of Benevento, respectively, in the same area of the 1990 sequence (Federici et al., 1992) with M_d less than 3.7 at depths less than 10 km. The fault plane solutions, showing normal faulting motions, can be divided into two groups with different orientations of maximum horizontal stress: one along the Apenninic chain and the other one along the E–W direction. The first swarm was correlated to an E–W surface lineament north of Benevento (Iannaccone et al., 1990) while the second one to a NNE–SSW structure transversal to Apennines chain (Federici et al., 1992).

After the 1992, sparse events and several swarms with small magnitudes (M_L ≤ 3.7) continually took place, but no detailed seismological studies exist.

4. Data and methods

4.1. Earthquake re-locations

The analyzed data were collected by three different seismic networks: the accelerometric National Strong Motion Network (RAN), managed by the Civil Protection Department, the broad-band and velocimetric Centralized National Seismic Network (RSNC), managed by the National Institute of Geophysics and Volcanology (INGV) and the velocimetric and accelerometric Irpinia Seismic Network (ISNet), owned by AMRA S.c.a.r.l. and operated by RISSC-Lab, the Seismological Laboratory of the Department of Physics at the University of Naples Federico II. For each network, we selected stations within 100 km from the epicenter in order to have the smallest azimuthal gap. The total number of selected stations is 33 (Fig. 1a).

The Benevento seismic sequence was composed by 40 events with M_L ranging between 1.3 and 4.1 (Fig. 2a). We manually picked the first P- and S-wave arrival times, assigning a weighting factor inversely proportional to the uncertainty in the pick (Supplementary Table S1). Also, we measured the P-wave polarity only for arrival times with time uncertainty smaller than 0.05 s. The number of measured P- and S-arrival times is 436 and 311, respectively (Fig. 2b). We used for the absolute locations a minimum of 3 P- and 1 S-wave arrival times within an epicentral distance of 50 km.

Before locating earthquakes, we checked the picking quality through the modified-Wadati diagram (Chatelain, 1978) whose correlation coefficient R^2 is 0.99 (Fig. 2c). Also, we estimated a Vp/Vs ratio of 1.78, which was then used in the earthquake location. This value falls between 1.73 and 1.82, which correspond to the range limits of Vp/Vs calculated in the same area by several authors (Alessio et al., 1996; Bisio et al., 2004; Improta et al., 2000; Milano et al., 1999).

Preliminary absolute locations were obtained using the NonLinLoc code (Lomax et al., 2000) that performs a global search to evaluate the earthquake location probability density function (PDF) with the Oct-Tree sampling procedure. This algorithm is more efficient giving an accurate and reliable mapping of the PDF with short computing times (e.g. Turino et al., 2009). We tested different local and regional 1-D velocity models (Alessio et al., 1996; Chiarabba and Amato, 1997; Chiarabba and Frepoli, 1997; Del Pezzo et al., 1983; Iannaccone et al., 1998; Improta et al., 2000; Fig. 2d). For the following analysis, we selected the model of Del Pezzo et al. (1983) that minimized both the rms on the arrival times and the location errors. Moreover, this model is also defined at larger depths as compared to the other models.

Then, we computed relative locations by applying a double-difference technique (HypoDD; Waldhauser and Ellsworth, 2000), that minimizes the residuals between observed and theoretical travel time differences (or double differences) for pairs of earthquakes at each station. We analyzed couples of events, for which the residual threshold for P and S absolute travel times is 0.05 s and whose hypocentral distance is smaller than 10 km. These constraints reduced the number of analyzed events to 28, using the absolute location as reference. Supplementary Fig. S3 displays the locations of the 2012

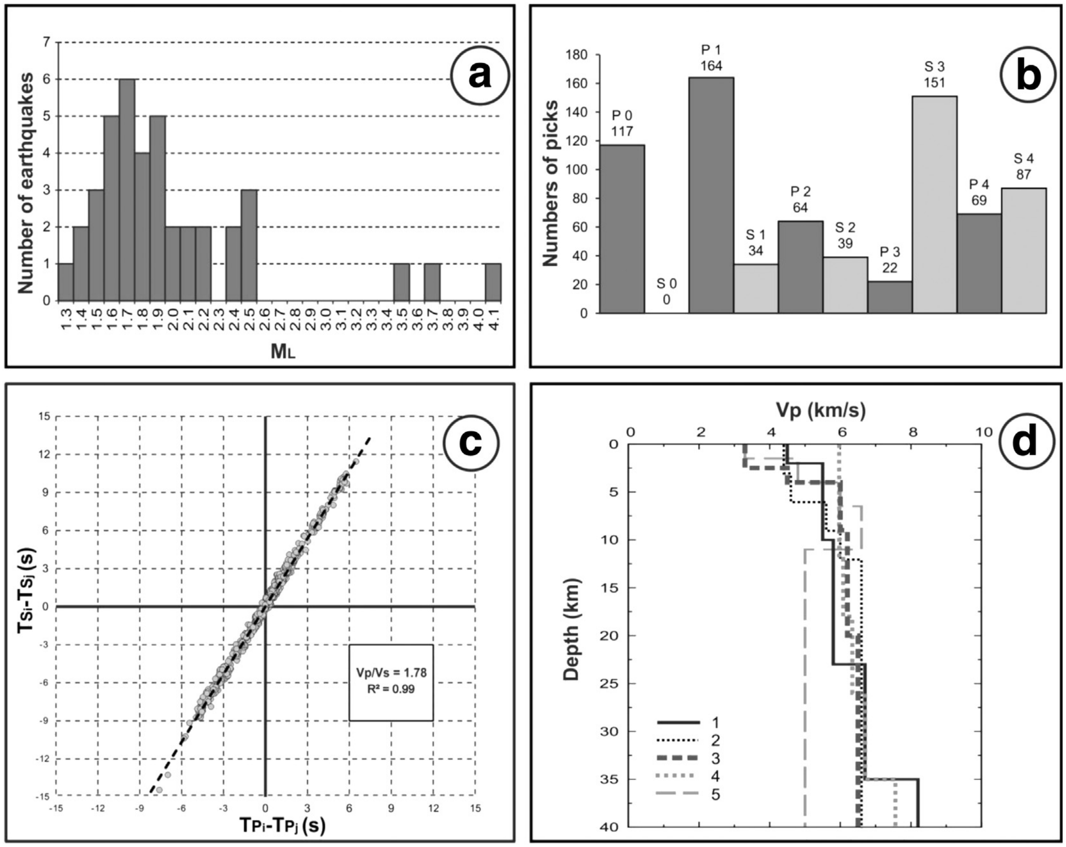

Fig. 2. a) Magnitude histogram of the 2012 Benevento seismic sequence (40 events). b) Number of P- and S-wave arrival times with their relative weight. c) Modified-Wadati diagram (Chatelain, 1978). d) 1-D velocity models tested during the preliminary earthquake absolute re-location. The velocity model selected for the complete analysis is the n.1 from Del Pezzo et al. (1983).
n.2 from Chiarabba and Amato (1997); n.3 from Alessio et al. (1996); n.4 from Chiarabba and Frepoli (1997); n. 5 from Iannaccone et al. (1998).

Benevento seismic sequence before and after the double-difference earthquake re-location technique.

The mean re-location errors are about 40 m (horizontal distance) and 50 m (vertical distance) respectively and the average rms is about 0.013 s by using singular value decomposition (SVD) method. The hypocentral distribution, located east of Benevento city, shows two seismic clusters (A and B in Fig. 3a–b–c) separated at about 2 km in horizontal extent and 1 km in a vertical section. No preferential alignment is evident also analyzing the hypocenter distribution for a single cluster. Events in the cluster A have a depth larger than 18 km. The cluster is composed by 14 events and includes the M_L 4.1 mainshock that started the sequence. The cluster B is shallower and located SE with respect to the cluster A. It is composed of 14 events (also containing the M_L 3.5 and M_L 3.7 earthquakes) whose depth ranges between 16 km and 18 km.

4.2. Refined source parameter estimates

Source parameters were estimated using a parametric approach combined with a multi-step, non-linear inversion strategy (Zollo et al., 2014). The observed S-wave displacement spectra were inverted assuming a Madariaga-type spectral model (Madariaga, 1976) with high-frequency decay proportional to $\omega^{-\gamma}$, and taking into account the correction for path attenuation and site response effects as in Zollo et al. (2014). The recorded signals were preliminary corrected for the instrument response considering for each station the specific transfer function of the sensor and the data logger. The S-wave displacement spectra were computed from the modulus of the two horizontal acceleration spectra by double integration in the frequency domain. The S waveforms were selected in a variable time-window bracketing the manual pick and depending on the analyzed earthquake local magnitude. For curve fitting and parameter estimate, the non-linear Levenberg–Marquardt least squares algorithm was used. After calculating the noise level in the whole frequency range, the signal-to-noise ratio at each frequency data was used as a weighting factor during the inversion of displacement spectra. We calculated the source parameters for the two major events (September 27, 01:08, M_w 4.3–M_L 4.1 and 08:35 M_w 3.9–M_L 3.7 earthquakes; hereinafter MS and AF2, respectively). After estimating the spectral parameters, as the low-frequency spectral level (Ω_0) and the corner frequency (f_c), the seismic moment M_0 and the source radius r were determined, considering a circular fault rupture according to the Madariaga (1976) source model. All the retrieved parameters are listed in Table 1.

4.3. Focal mechanisms

We retrieved the focal mechanism for the three main events by applying the Time Domain Moment Tensor full waveform inversion (TDMT, Dreger, 2003; Dreger and Helmberger, 1993; Scognamiglio et al., 2009). The algorithm inverts complete, three-component broadband displacement waveforms to estimate a point-source solution by fitting the synthetic seismograms to the observed data. We used broadband velocity waveforms recorded at all stations of the RSNC within 300 km from the earthquake epicenter. We extracted data in 800 s time windows starting 3 min before the event origin time; we corrected for the instrument response and we integrated to obtain the displacement records. Then, we resampled at 1 sps and finally band-pass filtered the signal in the frequency range 0.02–0.05 Hz for MS and AF2 events and in the 0.02–0.1 Hz range for M_L 3.5 aftershock (September 27, 03:47, M_L 3.5 aftershock; hereinafter AF1). The horizontal components

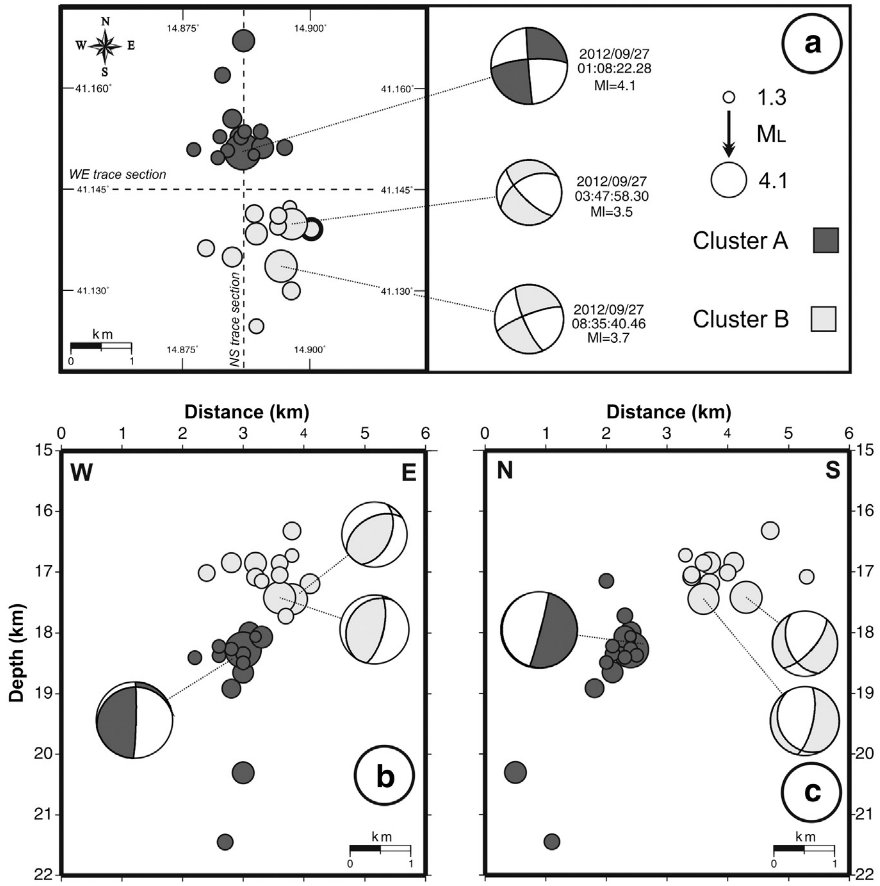

Fig. 3. Detail of the double difference earthquake re-locations of the 2012 Benevento earthquake in map (a) and along W–E (b) and N–S (c) trending vertical sections. The focal mechanisms are the Time Domain Moment Tensor fault plane solutions computed in this work. The M_L 2.2 earthquake, which occurred on September 27, 2012 at 01:23:04 (UTC) and was selected as EGF in the deconvolution technique of apparent source time functions, is highlighted with a black circle in panel (a).

were rotated to the transverse and radial ones. Green's functions were computed with the frequency–wavenumber integration method (Saikia, 1994) in the 1-D regional velocity model proposed by Scognamiglio et al. (2009).

After fixing the depth and the location of the earthquakes, the TDMT solutions were obtained discarding the data at stations with a poor waveform fit (VR < 10%, variance reduction parameter) to improve the quality of the solutions. For the MS, we inverted data from 12 stations obtaining a high quality solution, with a VR of 46% and a percentage of double couple (DC) of 97%. For the AF2 we got VR = 56% and DC = 87% from inversion of data from seven stations. We also achieved an acceptable solution for the AF1 event with a VR = 27% and DC = 66% using again seven stations (Table 2 and Supplementary Figs. S4–S5). The TDMT solutions of three largest events show a similar strike slip faulting with two high angle nodal planes striking roughly N–S and E–W. In particular, the MS shows a weak rotation (<10°) of nodal planes if compared with AF1 and AF2 (Fig. 3a). These events have the same nodal plane orientations with a lower dip angle; the difference is probably owing to the uncertainty of the solution considering the decrease in the signal-to-noise ratio.

Table 1
Estimated seismic source parameters. Madariaga (1976) source model is assumed for a circular fault rupture.

Date Origin time	M_w	M_0 *(Nm)*	f_c *(Hz)*	Crack radius *r (m)*
2012/09/27 01:08:22.280	4.3 ± 0.1	$(3.4 \pm 1.4) \times 10^{15}$	1.5	456
2012/09/27 08:35:40.460	3.9 ± 0.1	$(8.3 \pm 0.7) \times 10^{14}$	2.9	239

The retrieved solution for the mainshock is similar to the one published by the INGV (http://cnt.rm.ingv.it/tdmt.html#tdmt_references) and to the other one, calculated by Michele et al. (2014), while we used a larger number of stations. We finally superimpose the P-wave polarities to the focal mechanism as retrieved by the TDMT method (Supplementary Fig. S6). We found that most of the polarities agree with the focal solution. Several points fall in the vicinity of the nodal planes, while some of stations exhibit opposite polarities with respect to the focal solution. Moreover, the calculated focal mechanisms with the FPFIT code (Reasenberg and Oppenheimer, 1985), for events for which at least six P-wave first polarities, in this case strongly depend on the selected velocity model and show multiple solutions. However, among the best-fit solutions we also retrieved strike-slip type of faulting.

4.4. Kinematic rupture process analysis

We performed a kinematic rupture process analysis modeling the apparent source time functions (ASTFs) retrieved by waveforms data. The ASTFs were calculated by deconvolution of the impulse response of the medium from the recorded data, using the empirical Green's function (EGF) method (Hartzell, 1978). We adopted the deconvolution technique of Vallée (2004), which imposes the conditions of causality, positivity, limited duration and equal area as physical constraints on ASTFs. We selected as EGF the M_L 2.2 aftershock, which occurred on September 27, 2012 at 01:23:04 (UTC) and was recorded at a large number of stations, despite its magnitude (Fig. 3a). Then, we estimated the ASTFs at nine stations in the S-wave time window (Fig. 4).

We finally inverted the ASTFs to obtain a kinematic rupture model using the isochrone back-projection technique (Festa and Zollo, 2006).

Table 2
Moment tensor solutions for the three largest earthquakes of the 2012 Benevento sequence, obtained using the TDMT technique. Parameters used in the inversion are reported.

	Event #1	Event #2	Event #3
Date	2012/09/27	2012/09/27	2012/09/27
Origin time	01:08:22.280	03:47:58.30	08:35:40.460
$\mathbf{M_L}$	4.1	3.5	3.7
Latitude	41.150624	41.139835	41.133639
Longitude	14.886764	14.896445	14.894315
Depth *(km)*	18.285	17.441	17.417
Number of stations	12	7	7
Frequency band width *(Hz)*	0.02–0.05	0.02–0.1	0.02–0.05
Nodal planes *(strike/dip/rake)*	267/75/179	241/52/−157	250/78/−167
	177/89/−15	136/72/−40	158/78/−12
$\mathbf{T_{axis}}$ *(Plg/Azi)*	9/223	13/193	0/24
$\mathbf{N_{axis}}$ *(Plg/Azi)*	75/351	46/297	73/293
$\mathbf{P_{axis}}$ *(Plg/Azi)*	−11/131	41/92	17/114
Signal length *(s)*	175	175	175
Weighted reduced variance *(%)*	46.48	26.99	56.00
Double couple *(%)*	97.10	66.38	86.91
Compensated linear vector dipole *(%)*	2.90	33.62	13.09
Quality *(after Scognamiglio et al., 2009)*	Ba	Ca	Ba

The method back projects the amplitudes of ASTFs along the isochrone curves on the fault plane, to retrieve the slip distribution associated to a single receiver and stacks the retrieved maps to obtain the final kinematic model. After testing different rupture velocities, we selected the final kinematic model that minimizes the L1-norm between synthetic and observed ASTF waveform amplitudes (Fig. 5a). In this analysis, the fault geometry was fixed at the solution derived from the TDMT inversion with a strike 267° and dip 75° in the north direction.

In order to discriminate the fault plane for the largest event in the sequence, we analyzed the ASTFs exploring the directivity effect. ASTFs of BENI and SGTA stations clearly show a different duration at opposite azimuths roughly along the E–W nodal plane (Fig. 4). Since the ASTF

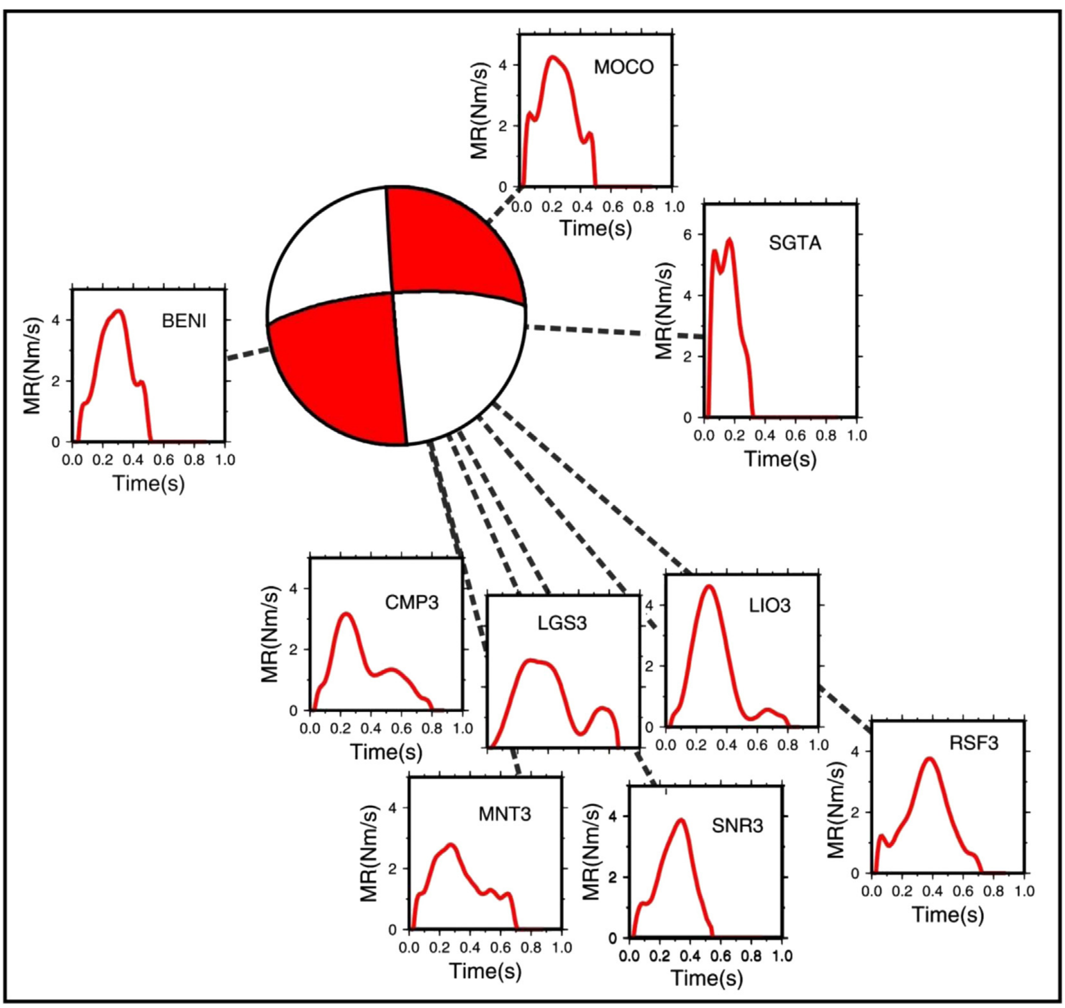

Fig. 4. Retrieved ASTFs for the mainshock of 2012 Benevento sequence. The ASTFs are arranged along the azimuths of the stations with respect to the location of 2012 Benevento mainshock. The moment rate (MR) unit is 1×10^{15} Nm/s. TDMT focal mechanism solution is also reported.

Please cite this article as: Adinolfi, G.M., et al., The September 27, 2012, M_L 4.1, Benevento earthquake: A case of strike-slip faulting in Southern Apennines (Italy), Tectonophysics (2015), http://dx.doi.org/10.1016/j.tecto.2015.06.036

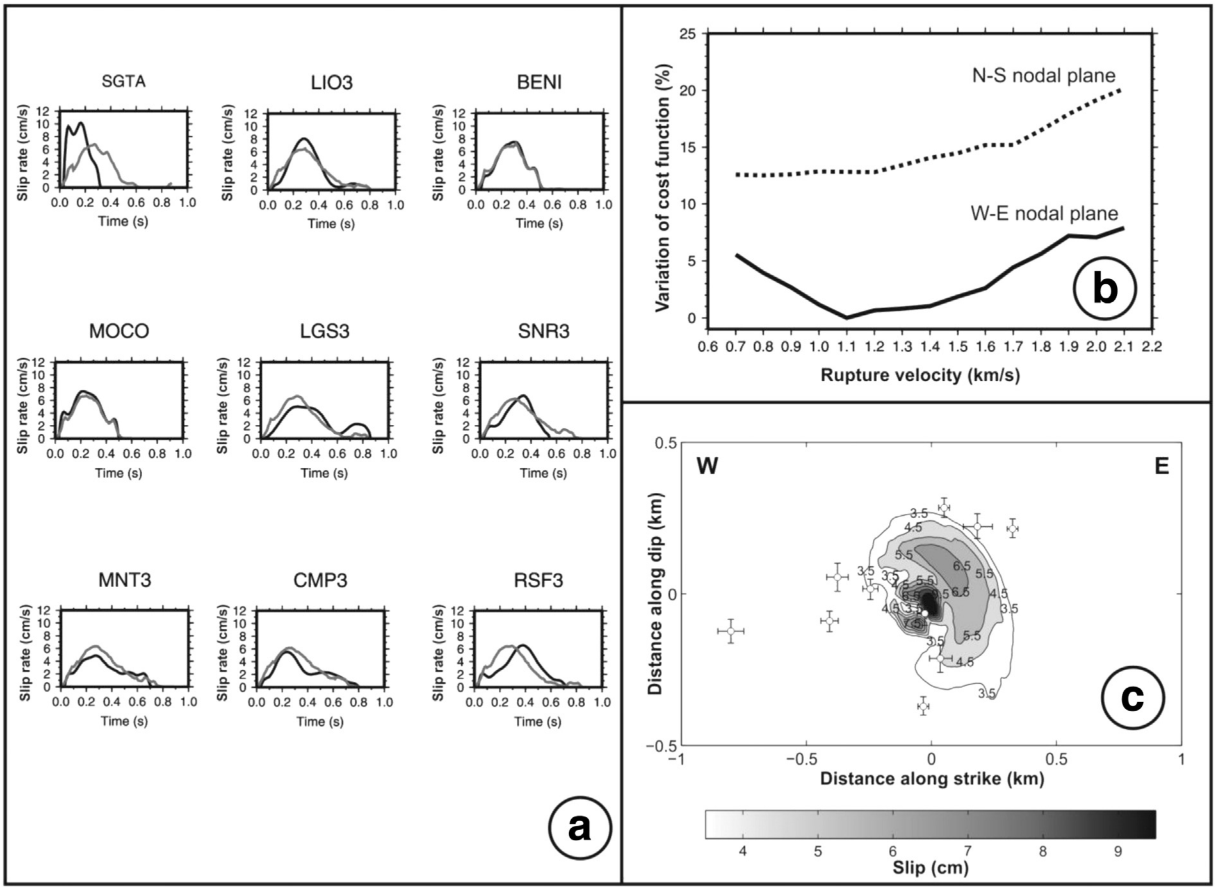

Fig. 5. a) Comparison between synthetic (gray lines) and observed (black line) ASTF waveforms for each station used in the analysis. b) Percentage variation of the normalized cost function versus the rupture velocity for both the mainshock nodal planes. The absolute minimum was obtained for the nodal plane with strike 267° and dip 75° (roughly E–W nodal plane), for a rupture velocity of 1.3 km/s. c) Slip map of the mainshock and the cluster A events of the 2012 Benevento sequence projected onto the fault plane. Horizontal and vertical location errors are also displayed.

at BENI is characterized by a longer duration and lower amplitude as compared to SGTA, we may argue that the main rupture propagated along the E–W plane, from west to east. Looking at the remaining ASTFs, no directivity effect is clear for a potential N–S striking conjugate plane.

We also investigated which plane was responsible for the rupture using the isochrone back-projection technique. We assumed a constant rupture velocity whose value ranges between 1.0 and 2.5 km/s. Comparing the misfit for the two planes for different values of the rupture velocity, the E–W trending, rupture plane is well constrained. In Fig. 5b, we plotted the difference between the actual misfit function and the misfit value for the minimum normalized by this latter value. This quantity measures the relative difference between a generic misfit and the minimum value and is represented in Fig. 5b in a percent scale. The nodal plane with strike 267° and dip 75.4° shows a curve whose trend is constantly smaller than the values for the other plane of a quantity between 10 and 15%. This result indicates that the ASTFs discriminate the fault plane with a significant reduction of the misfit function. For the E–W plane, the rupture velocity value, for which the misfit is minimum, is 1.3 km/s (Fig. 5b). Nevertheless, the small percentage variation (≤8%) of the cost function in the whole explored range and the flattening of the function around the minimum indicate a large uncertainty, although smaller values better describe the evolution of the ASTFs.

The retrieved slip map shows a relatively complex pattern in good agreement with the estimated fracture size. The slip is mainly concentrated in two patches of different sizes, shapes and slip values: the smallest one shows the largest average slip, around the nucleation region while the other one has a larger size and is located north-east on the fault plane (Fig. 5c). The fracture propagated toward east and in the up-dip directions along the fault plane, which explains the evidence for directivity effect as revealed by ASTFs at BENI and SGTA (Fig. 4). Additionally, analyzing the shape of ASTFs, they show a rapid increase toward the peak value: this trend is associated to the large slip patch close to the nucleation region where the propagating rupture quickly reaches the zone of the largest dislocation (Fig. 5a–c).

Finally, we also projected all the aftershocks of cluster A onto the main-shock fault plane. Aftershocks are often concentrated at the boundaries of the main rupture or along structural complexities crossed by the main rupture (Scholz, 2002). Although there are only few aftershocks for the cluster A to be considered, it is clear that most of them are concentrated in minimum or no-slip zones underlying structural zone of larger shear strength. One group is located at the borders of the large slip patch indicating the eastern part of the rupture area as structurally complex. We argue that these aftershocks were generated by static stress transfer, associated to the main rupture propagation.

5. Discussion and seismotectonic interpretation

The relocated 2012 Benevento seismic source lies at depths between 16 and 20 km, nearly 10 km eastward from the town of Benevento. The seismogenic fault plane, referred later to as Benevento mid-crust fault (e.g. BMCF) consists of two distinct seismogenic fault segments activated during the seismic sequence. The MS and AF2 produced an almost circular rupture with a radius of about 450 m and 240 m, respectively. As derived from the integrated analyses of the hypocentral distribution (Fig. 3) and the mainshock focal mechanism geometry (strike 267° and dip 75°), the reconstructed seismogenic plane dips at 75° NNW and is characterized by a nearly pure right-lateral strike-slip kinematics (rake 179°).

Bearing in mind the retrieved slip map, the fracture size, the earthquake re-location and the geometrical constraints, we argue that the seismicity clustered onto two small fault segments activated during the seismic sequence. Cluster A seismicity developed along a deeper, subvertical dextral strike slip fault segment with a strike around 267° and dip 75° in the north direction. Cluster B took place along a different, shallower dextral strike slip plane portion, with strike of about 250° and dip 78° to the north. Almost the same number of events with comparable magnitude has composed the two clusters. This result was also confirmed by source parameter estimates. The largest event in the sequence had a seismic moment and source radius equal $(3.4 \pm 1.4) \times 10^{15}$ Nm and 450 m, respectively (Table 1). As indicated by their relative locations and the rupture size, the AF1 and the AF2 do not occur in the mainshock focal region (Fig. 3a), indicating the existence of two distinct seismicity clusters each of them with its own mainshock–aftershock evolution.

As for other low energy seismic sequences, the earthquakes are concentrated in the foci zone of each fault segment and do not show any preferential alignment. An east propagating fracture for the main event of the cluster A may instead have triggered the cluster B on a different fault segment almost parallel to the first one. The static stress change generated by the MS event should be responsible of the activation of the adjacent fault portion along which the cluster B occurred through a mechanism of stress transfer to the southeast and up dip directions. As shown in Supplementary Fig. S7, the seismicity temporal evolution should corroborate this idea.

The BMCF is located beneath the axial sector of the Apennines mountain chain, within the Apulian foreland mid-crust in the footwall of the easternmost Apennines thrust system. This compressional system (outer thrust system) was active from the Late Pliocene to 0.65 Ma ago and is considered to be presently inactive (Boncio et al., 2007; Menardi Noguera and Rea, 2000; Patacca and Scandone, 2001). The prevailing seismogenic deformation field in the Sannio epicentral area of the Benevento 2012 sequence is of the extensional type, as testified by both the background seismicity (e.g., 1990 and 1991–92 sequences; Alessio et al.,

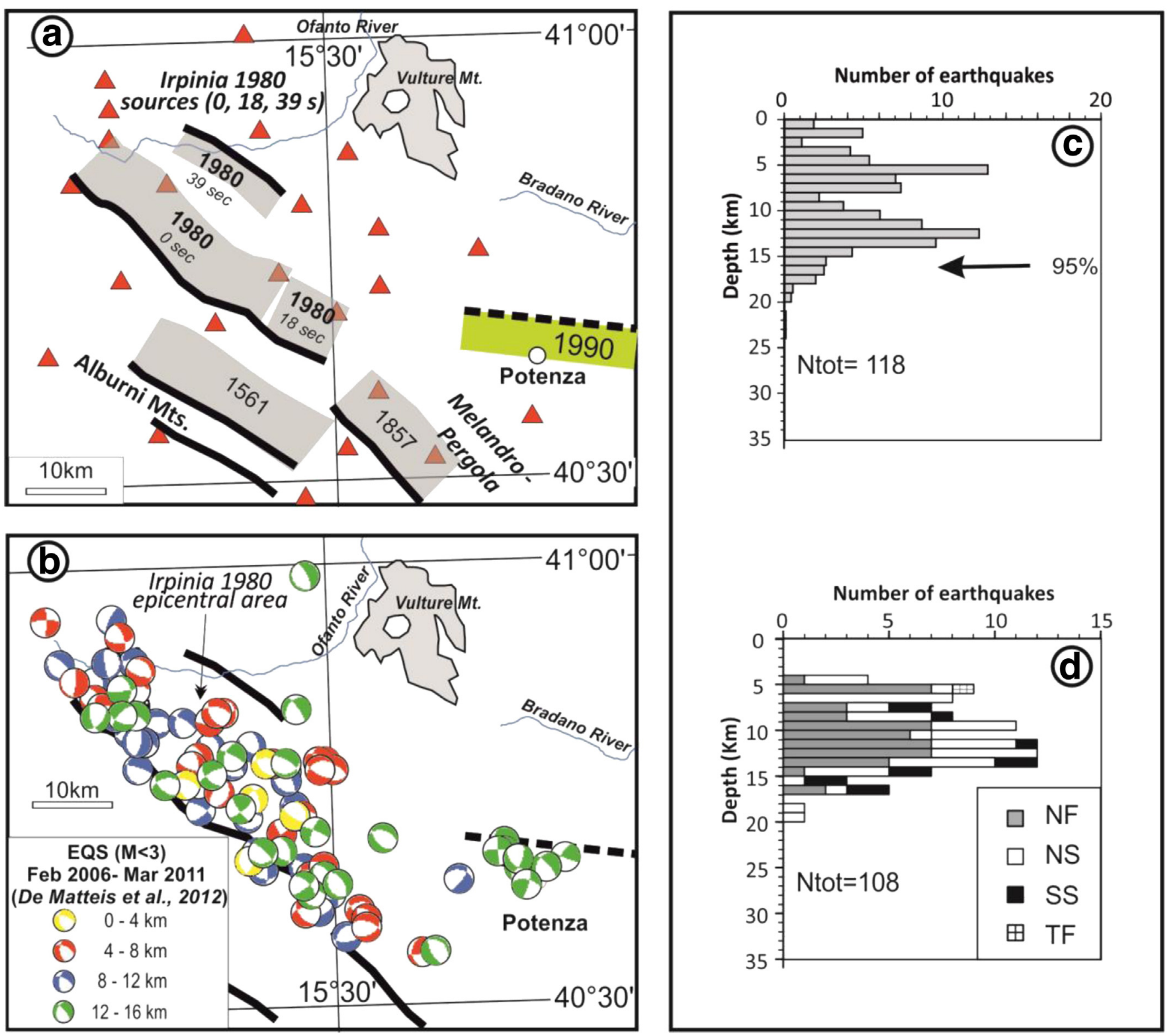

Fig. 6. a) Detail of seismogenic master faults and box-shaped source (modified from DISS Working Group, 2010) of the major historical and instrumental earthquakes within the area covered by the ISNet — Irpinia Seismic Network (triangle symbols). b) and c) Focal mechanisms and seismicity frequency–depth distribution for the Irpinia and Potenza areas. The data are derived from De Matteis et al. (2012). d) Earthquake focal mechanisms from De Matteis et al. (2012) and frequency–depth distribution of fault plane solution organized in kinematic classes as in Frohlich (1992). Key: NF, normal fault; NS, normal-oblique; SS, strike-slip; TF, thrust fault kinematics.

Please cite this article as: Adinolfi, G.M., et al., The September 27, 2012, M_L 4.1, Benevento earthquake: A case of strike-slip faulting in Southern Apennines (Italy), Tectonophysics (2015), http://dx.doi.org/10.1016/j.tecto.2015.06.036

1996; Federici et al., 1992) and the most relevant instrumental earthquakes, such as the 1962 earthquake. As in Central Apennines (Ferrarini et al., 2015), the extensional field extends with continuity from the area of the 1984 Barrea earthquake, to the north, to the Irpinia area, to the south, with a common average SW–NE direction of the T-axes derived from focal mechanisms. As far as it concerns the Irpinia area, good quality data are also available for Apennines background seismicity (De Matteis et al., 2012). The seismicity is located along the chain where the sources of major historical and instrumental earthquakes are identified (Fig. 6). The depth histogram of Fig. 6c shows that 95% of the seismic events occurred, with nearly uniform distribution, in the uppermost 15 km of the crust. The focal mechanisms, ranging between pure-normal and normal-strike kinematics, indicate a dominant SW–NE extensional regime (Fig. 6b–d). Hence, the background low magnitude seismicity and the related stress field are closely linked with the major fault segments activated during the M_s 6.9 1980 earthquake: three main rupture episodes at 0, 18, and 39 s after the first shock involved approximately 60-km long NW–SE striking fault segments with a pure normal kinematic (Bernard and Zollo, 1989; Pantosti and Valensise, 1990; Westaway and Jackson, 1987) (Fig. 6a).

Conversely, we observe interesting seismotectonic similarities between the 2012 Benevento sequence and both the 1990–1991 Potenza and Molise 2002 earthquakes, in terms of analogous structural position, fault geometry and kinematics. The Potenza seismic sequence released a M_w 5.7 event on May 5, 1990 and a M_w 5.2 event on May 26, 1991. Both events and most of their aftershocks were originated by an E–W-striking dextral strike-slip fault located in the footwall of the easternmost Apennines thrust system, within the Apulian foreland crust. The seismicity was concentrated within the crystalline basement at middle crust depths between 15 and 25 km (Boncio et al., 2007; Di Luccio et al., 2005b) (Fig. 7a). The recent background seismicity confirms the above pattern showing a roughly E–W alignment with depths up to 25 km, focal mechanisms with dominant dextral strike-slip motion and a prevalent strike-slip tectonic regime (De Matteis et al., 2012) (Fig. 6b–d). The Molise seismic sequence released two M_w 5.7 events on October 31 and November 1, followed by a long aftershock sequence. A buried E–W trending fault system, consisting of two en-echelon segments with a total length of 15 km, was outlined by earthquake distribution, mainly at depths between 10 and 25 km (Fig. 7b). Similar to the 1990 Potenza earthquakes, the 2002 Molise seismic sequence was originated by multiple ruptures along E–W striking right lateral fault (Chiarabba et al., 2005; Di Luccio et al., 2005a). The seismicity was concentrated below the bottom of the carbonate sedimentary cover, within the Apulian foreland middle crust.

Several authors (Boncio et al., 2007; Di Bucci and Mazzoli, 2003; Di Bucci et al., 2006; Di Luccio et al., 2005b; Valensise et al., 2004) have interpreted the Molise and Potenza seismicity as the deep seismogenic expression of active right-lateral strike-slip faults that dissect the Apulia foreland. Such structures may be interpreted as crustal-scale E–W-striking fault zones, possibly inherited from previous tectonic phases and reactivated under the present-day deformation field. The seismogenic fault zones activated in instrumental times are located at mid-crustal levels, but they appear in physical continuity with outcropping structures, such as the case of 2002 Molise fault zone and the active Mattinata fault well exposed in the Gargano promontory (e.g. Di Bucci et al., 2010).

Summarizing, our detailed analysis of the 2012 Benevento sequence and its interpretation in the regional framework provide some constraints for the definition of the seismotectonic setting of the Southern Apennines (Fig. 8).

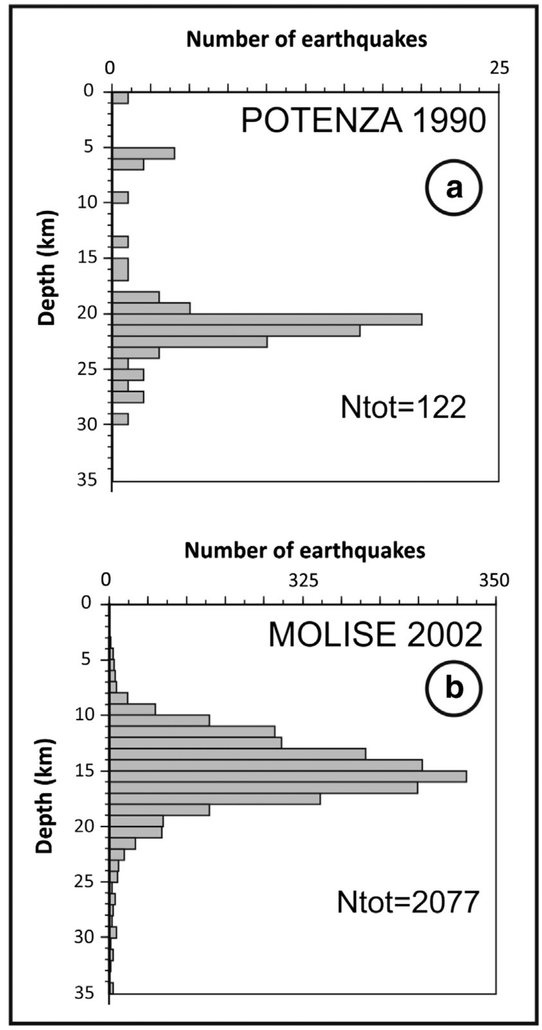

Fig. 7. Depth–distribution of the selected events (qualities A and B) occurred during the 1990 Potenza seismic sequence (a; $0.6 \le M_d \le 3.1$, $M_{w\text{-}max}$ 5.7) and during the 2002 Molise seismic sequence (b; $2.0 \le M_L \le 4.2$, $M_{w\text{-}max}$ 5.7) as derived from Boncio et al. (2007) and from Chiarabba et al. (2005), respectively.

1. A buried NNW-dipping high-angle source is identified at mid-crust beneath the Benevento extensional area. It might represent a small portion of a much larger fault source. We have no constrains about the extent of the Benevento mid-crust fault zone, its tectonic importance and the maximum magnitude that it should be capable to generate. Nevertheless, for this reason, it is very crucial to pay special attention to Benevento area, where the presence of a strike-slip zone very similar to the Potenza and Molise ones, as supposed by this study, should affect its already high seismic hazard. It is worth to note that the reconstructed Benevento source would lie along the E–W striking source activated by the earliest mainshock of the December 5, 1456 sequence, according to the Fracassi and Valensise (2007) interpretation of the macroseismic field.
2. The strong similarities among 2012 Benevento, 1990–1991 Potenza and the 2002 Molise seismic sequences are evident not only in terms of fault kinematics and focal depths, but also in terms of the architecture of the host crustal structure. The Benevento earthquake crucial location corroborates the idea of the existence of the same seismotectonic environment of regional importance across the whole Apulian foreland crust. It is characterized by a thick seismogenic crustal layer that gradually deepens westward, from the outcropping Apulian foreland to the Apennines chain. It includes both the sedimentary upper crust and the underlying middle crust, confined at the footwall of the outer basal thrust of the Apennines compressional system. A strike-slip regime, exclusively confined beneath the basal thrust and along discrete E–W deformation zone, can produce seismicity both at shallow depths in the most external sectors (e.g. outcropping Mattinata fault) and at deeper crustal level (>15 km) toward the Apennines units, such as like the 2012

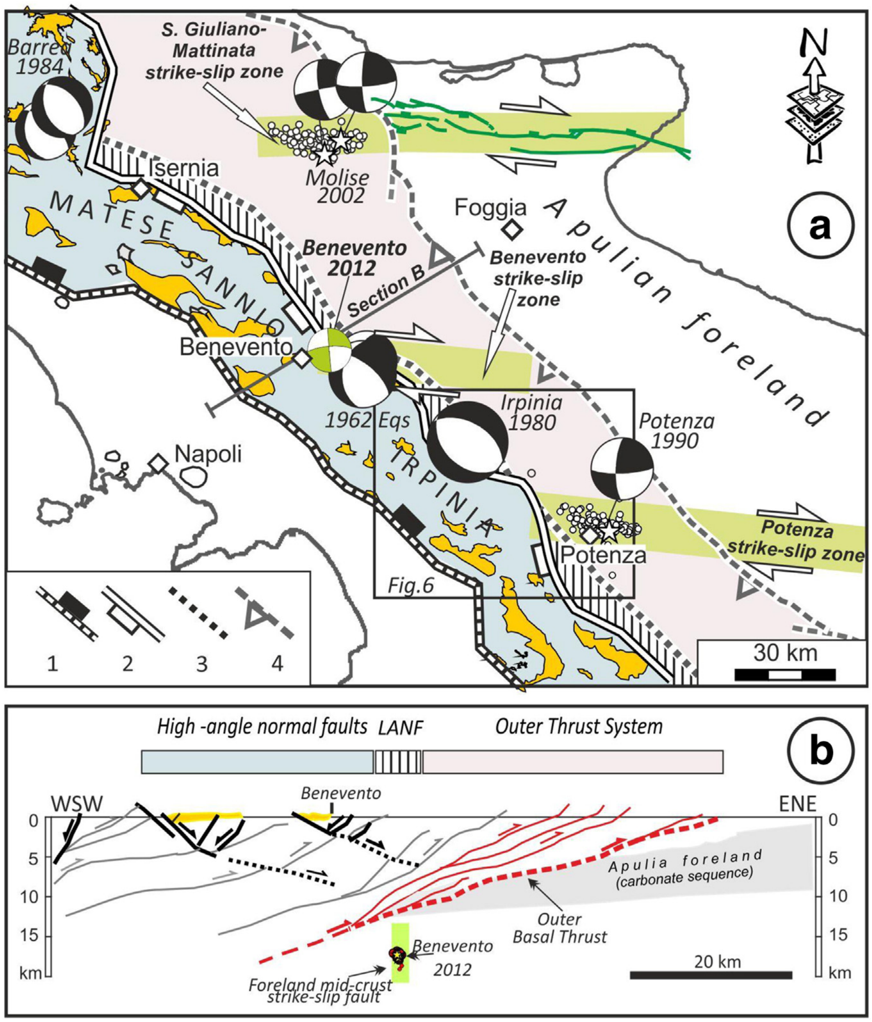

Fig. 8. a) Schematic seismotectonic zoning of Southern Italy with location of the Irpinia — ISNet study area of Fig. 6 and trace of the interpretative section. The epicenter locations of 1990–1991 Potenza (M_w 5.7) and Molise 2002 (M_w 5.7) seismic sequences are reported (Boncio et al., 2007; Chiarabba et al., 2005). The fault plane solutions are derived from European–Mediterranean Regional Centroid Moment Tensor (RCMT) Catalogue. Key: 1, major E-NE dipping normal faults; 2, major W-SW dipping normal faults; 3, buried outer limit of low angle normal faults (LANFs); 4, buried front of the Apennines chain. b) Interpretative section along the trace of section n.6 in Mostardini and Merlini (1986) across the Southern Apennines; the surface structure and the style of the extensional deformation are from Brozzetti (2011).

Benevento, the 1990–1991 Potenza and the 2002 Molise earthquakes (Fig. 8).

3. Conversely from what was proposed for the Northern-Central Apennines (Elter et al., 2011), up to now, no meaningful and consistent strike-slip sequence has been observed and studied in the axial sector of the Apennines belt of Southern Italy. Here, on the other hand, the prevailing kinematics is extensional, as shown by both background seismicity and large events, such as the 1962 and the 1980 Irpinia earthquakes.
4. The 2012 Benevento earthquake case suggests a potential vertical seismotectonic zonation of the Southern Apennines. The intra-Apennines area is undergoing extension that may produce NW–SE seismogenic faulting in the brittle shallow crust (10–12 km thick) (see histograms in Fig. 6c–d) consistent with large to moderate seismicity recorded along the mountain axial zone, like the 1980 Irpinia earthquake. In the footwall under the Apennines outer basal thrust (Fig. 8b), the present strike-slip stress field might reactivate inherited E–W-striking crustal (or possibly lithospheric) fault zones depending strongly on the rheological stratification that can produce a discontinuous mechanical behavior along-dip (Boncio et al., 2007).
5. The axial belt of Southern Apennines of Italy appears to be characterized by the coexistence of two different stress regimes, vertically overlapping, a shallow extensional one (<15 km) and a deep transcurrent one (20–25 km) with a common SW–NE direction of the least principal stress. In our opinion, the vertical transition between the two regimes does not appear to be gradual and simply controlled by an interchange with depth of σ_1 with σ_2 from a vertical to a sub-horizontal direction. It rather looks to be tectonically controlled. In fact, the strike-slip regime deepens westward and remains confined at the footwall of outermost SW-dipping basal thrust of the Apennines fold-and-thrust belt (Fig. 8b). This idea, which cannot be completely considered a result of our work, is suggested by several stress regime studies of the Apulian crust (De Matteis et al., 2012; Montone et al., 2012; Pierdominici and Heidbach, 2012) and, partially, by our analysis. Moreover, the superposition of different stress regimes is common to other sectors of the Apennines, as the western portion of the Northern Apennines (Eva et al., 2005).
Beyond the interpretation, the effective reason (differential rheological behavior, large scale tectonic processes, etc.) of stress change in this area remains unconstrained, and should be the object of future investigation.

6. Conclusions

In this paper we performed a complete rupture analyses of a recent small intra-Apennines sequence (September 27–30, 2012; M_{Lmax} 4.1),

Please cite this article as: Adinolfi, G.M., et al., The September 27, 2012, M_L 4.1, Benevento earthquake: A case of strike-slip faulting in Southern Apennines (Italy), Tectonophysics (2015), http://dx.doi.org/10.1016/j.tecto.2015.06.036

which occurred close to the town of Benevento, in one of the most seismic active areas of the Southern Apennines extensional belt (Italy). In spite of its low magnitude, the sequence is interesting from a seismotectonic point of view due to its kinematics (e.g. strike-slip) and depth (e.g. mid-crust), which do not recall the upper crust extensional geometry of the neighboring epicentral events, but is rather similar to that of the far-away strike-slip earthquakes within the Apulian foreland (e.g. 1990–1991 Potenza 1990 and 2002 Molise).

- High precision earthquake re-location and focal mechanisms reveal an unknown high-angle dipping seismogenic source (BMCF) seated at mid-crust (16–20 km) nearby Benevento (10 km eastward). The main seismogenic plane dips 75° NNW with a strike of 267° and is characterized by a nearly pure right-lateral strike-slip kinematics (rake 179°).
- Considering the mainshock fracture size (radius 450 m) and the geometrical constrains, two near small fault segments were activated during the 2012 Benevento seismic sequence. Each fault segment produced an earthquake cluster (here called clusters A and B) whose occurrence was likely related to a static stress transfer mechanism taking into account an east and up-dip propagating fracture.
- The kinematic rupture analysis constrains the roughly E–W striking fault plane and underlines its complex structure. Considering the time duration and the relative amplitude, ASTFs at BENI and SGTA seismic stations clearly show a directivity effect due to an eastward-propagating rupture along the fault plane. This result is also verified by the remaining ASTFs that were inverted in a slip map consistent with an east- and up-dip migrating rupture. During the mainshock (M_w 4.3), the slip was mainly concentrated into two patches of different sizes and amplitudes located around the nucleation region and to the NE. The smallest one shows a maximum slip value of 9.5 cm, the other one of 7 cm.
- Taking into account the strong similarities with the 1990–1991 Potenza and 2002 Molise earthquakes, the BMCF seismicity suggests a strike-slip regime confined at the footwall of the outer basal thrust of the Apennines compressional system, that gradually deepens westward from the outcropping Apulian foreland to the axial chain.

In conclusion, our work suggests a reliable and robust approach to investigate the background seismicity, especially when it is spatio-temporally arranged in seismic swarms or sequences. A detailed seismological analysis of seismic sequences, taking into consideration also the rupture process study and kinematic slip inversion, is required to collect as many information as possible to better understand the seismotectonics of the analyzed area.

Data and resources

1. The instrumental seismicity is from the Italian Seismicity Catalogue (CSI) available at http://csi.rm.ingv.it/ and from the Italian Seismological Instrumental and Parametric Data-Base (ISIDE) available at http://iside.rm.ingv.it/iside/standard/index.jsp; the historical seismicity is available at http://emidius.mi.ingv.it/CPTI/ (last accessed 1 June, 2014).
2. Focal mechanism solutions are partially extracted from Regional Centroid Moment Tensor (RCMT) catalogue, available at http://www.bo.ingv.it/RCMT/ (last accessed 1 June, 2014).

Acknowledgments

This work was financed by DiS.P.U.Ter, University of Chieti "G. d'Annunzio" (research funding to Giusy Lavecchia) and by Department of Physics, University of Naples "Federico II" (research funding to Aldo Zollo). We thank the DPC (Italian Civil Protection Department) and the INGV (Italian National Institute of Geophysics and Volcanology) for data exchange. Special thanks go to Francesco Brozzetti, for comments and for the schematic structural map of Southern Italy used in this work, and to Martin Vallée, for the source code used to compute the ASTFs. We gratefully acknowledge the Editor Jean-Philippe Avouac and three anonymous reviewers for the useful and constructive comments that helped to improve the original manuscript.

Appendix A. Supplementary data

Supplementary data to this article can be found online at http://dx.doi.org/10.1016/j.tecto.2015.06.036.

References

Alessio, G., Gorini, A., Vilardo, G., Iannaccone, G., 1996. Low energy sequences in areas with high seismic potential: Benevento (Southern Apennines), April 1990. In: Schenk, V. (Ed.), Advances in Natural and Technological Hazard Research—Earthquake Hazard and Risk. Kluwer Academic Publishers, Dordrecht, pp. 3–16.

Basili, R., Valensise, G., Vannoli, P., Burrato, P., Fracassi, U., Mariano, S., Tiberti, M., Boschi, E., 2008. The database of individual seismogenic sources (DISS), version 3: summarizing 20 years of research on Italy's earthquake geology. Tectonophysics 453, 20–43.

Bernard, P., Zollo, A., 1989. The Irpinia (Italy) 1980 earthquake: detailed analysis of a complex normal faulting. J. Geophys. Res. 94, 1631–1647. http://dx.doi.org/10.1029/JB094iB02p01631.

Billi, A., 2003. Solution slip and separations on strike-slip fault zones: theory and application to the Mattinata Fault, Italy. J. Struct. Geol. 25, 703–715. http://dx.doi.org/10.1016/S0191-8141(02)00077-9.

Bisio, L., Di Giovambattista, R., Milano, G., Chiarabba, C., 2004. Three-dimensional earthquake locations and upper crustal structure of the Sannio–Matese region (Southern Italy). Tectonophysics 385 (1–4), 121–136.

Boncio, P., Mancini, T., Lavecchia, G., Selvaggi, G., 2007. Seismotectonics of strike-slip earthquakes within the deep crust of southern Italy: geometry, kinematics, stress field and crustal rheology of the Potenza 1990–1991 seismic sequences (Mmax 5.7). Tectonophysics 445, 281–300.

Brozzetti, F., 2011. The Campania–Lucania Extensional Fault System, southern Italy: a suggestion for a uniform model of active extension in the Italian Apennines. Tectonics 30, TC5009.

Butler, R.W., Corrado, S., Mazzoli, S., De Donatis, M., Di Bucci, D., Naso, G., Zucconi, V., 2000. Time and space variability of «thin-skinned» and «thick-skinned» thrust tectonics in the Apennines (Italy). Rend. Lincei 11 (1), 5–39.

Castello, B., Selvaggi, G., Chiarabba, C., Amato, A., 2006. CSI Catalogo della sismicità italiana 1981-2002, versione 1.1. INGV-CNT. Roma http://csi.rm.ingv.it/.

Cavazza, W., Roure, F., Ziegler, P.A., 2004. The Mediterranean area and the surrounding regions: active processes, remnants of former Tethyan oceans and related thrust belts. The TRANSMED Atlas. The Mediterranean Region From Crust to Mantle. Springer, Berlin Heidelberg, pp. 1–29.

Chatelain, J.L., 1978. Etude fine de la sismicité en zone de collision continentale au moyen d'un réseau de stations portables: la région Hindu-Kush Pamir (Doctoral dissertation) Université Scientifique et Médicale de Grenoble.

Chiarabba, C., Amato, A., 1997. Upper-crustal structure of the Benevento area (Southern Italy): fault heterogeneities and potential for large earthquakes. Geophys. J. Int. 130, 229–239.

Chiarabba, C., Frepoli, A., 1997. Minimum 1D velocity models in Central and Southern Italy: a contribution to better constrain hypocentral determinations. Ann. Geophys. 40 (4).

Chiarabba, C., De Gori, P., Chiaraluce, L., Bordoni, P., Cattaneo, M., De Martin, M., Frepoli, A., Michelini, A., Monachesi, A., Moretti, M., Augliera, G.P., D'Alema, E., Frapiccini, M., Gassi, A., Marzorati, S., Di Bartolomeo, P., Gentile, S., Govoni, A., Lovisa, L., Romanelli, M., Ferretti, G., Pasta, M., Spallarossa, D., Zunino, E., 2005. Mainshocks and aftershocks of the 2002 Molise seismic sequence, southern Italy. J. Seismol. 9, 487–494.

Cinque, A., Patacca, E., Scandone, P., Tozzi, M., 1993. Quaternary kinematic evolution of the Southern Apennines. relationships between surface geological features and deep lithospheric structures. Ann. Geophys. 36 (2).

De Matteis, R., Matrullo, E., Rivera, L., Stabile, T.A., Pasquale, G., Zollo, A., 2012. Fault delineation and regional stress direction from the analysis of background microseismicity in the southern Apennines, Italy. Bull. Seismol. Soc. Am. 102 (4), 1899–1907.

Del Pezzo, E., Iannaccone, G., Martini, M., Scarpa, R., 1983. The 23 November 1980 southern Italy earthquake. Bull. Seismol. Soc. Am. 73, 187–200.

Di Bucci, D., Mazzoli, S., 2003. The October–November 2002 Molise seismic sequence (southern Italy): an expression of Adria intraplate deformation. J. Geol. Soc. 160 (4), 503–506.

Di Bucci, D., Ravaglia, A., Seno, S., Toscani, G., Fracassi, U., Valensise, G., 2006. Seismotectonics of the southern Apennines and Adriatic foreland: insights on active regional E–W shear zones from analogue modeling. Tectonics 25 (4).

Di Bucci, D., Burrato, P., Vannoli, P., Valensise, G., 2010. Tectonic evidence for the ongoing Africa–Eurasia convergence in central Mediterranean foreland areas: a journey among long-lived shear zones, large earthquakes, and elusive fault motions. J. Geophys. Res. Solid Earth (1978–2012) 115 (B12).

Di Luccio, F., Fukuyama, E., Pino, N.A., 2005a. The 2002 Molise earthquake sequence: what can we learn about the tectonics of southern Italy? Tectonophysics 405 (1), 141–154.

Di Luccio, F., Piscini, A., Pino, N.A., Ventura, G., 2005b. Reactivation of deep faults beneath southern Apennines: evidence from the 1990–1991 Potenza seismic sequences. Terra Nova 17, 586–590. http://dx.doi.org/10.1111/j.1365-3121.2005.00653.x.

Dreger, D.S., 2003. 85.11 TDMT_INV: time domain seismic moment tensor inversion. Int. Geophys. 81, 1627.

Dreger, D.S., Helmberger, D.V., 1993. Determination of source parameters at regional distances with three-component sparse network data. J. Geophys. Res. Solid Earth (1978–2012) 98 (B5), 8107–8125.

Elter, F.M., Piero, E., Claudio, E., Elena, E., Katharina, K.R., Matteo, P., Stefano, S., 2011. Strike-slip geometry inferred from the seismicity of the Northern-Central Apennines (Italy). J. Geodyn. 52 (5), 379–388.

Eva, E., Ferretti, G., Solarino, S., 2005. Superposition of different stress orientations in the western sector of the northern Apennines (Italy). J. Seismol. 9 (4), 413–430.

Federici, P., Di Maro, R., Marchetti, A., Cocco, M., 1992. Analisi della sismicità dell'area del Sannio–Matese negli anni 1991–1992. Atti dell'XI Convegno Annuale GNGTS, CNR, Roma I, pp. 389–404.

Ferrarini, F., Lavecchia, G., de Nardis, R., Brozzetti, F., 2015. Fault geometry and active stress from earthquakes and field geology data analysis: the Colfiorito 1997 and L'Aquila 2009 Cases (central Italy). Pure Appl. Geophys. 172 (5), 1079–1103.

Festa, G., Zollo, A., 2006. Fault slip and rupture velocity inversion by isochrone backprojection. Geophys. J. Int. 166 (2), 745–756.

Fracassi, U., Valensise, G., 2007. Unveiling the sources of the catastrophic 1456 multiple earthquake: hints to an unexplored tectonic mechanism in southern Italy. Bull. Seismol. Soc. Am. 97 (3), 725–748.

Frohlich, C., 1992. Triangle diagrams: ternary graphs to display similarity and diversity of earthquake focal mechanisms. Phys. Earth Planet. Inter. 75, 193–198.

Gorini, A., Nicoletti, M., Marsan, P., Bianconi, R., de Nardis, R., Filippi, L., Marcucci, S., Palma, F., Zambonelli, E., 2010. The Italian strong motion network. Bull. Earthq. Eng. 8, 1075–1090.

Hartzell, S.H., 1978. Earthquake aftershocks as Green's functions. Geophys. Res. Lett. 5 (1), 1–4.

Hauksson, E., Shearer, P., 2005. Southern California hypocenter relocation with waveform cross-correlation, part 1: results using the double-difference method. Bull. Seismol. Soc. Am. 95, 896–903. http://dx.doi.org/10.1785/0120040167.

Iannaccone, G., Romeo, R., Tranfaglia, G., Errico, L., Lentini, E., Bernard, P., et al., 1990. Analisi della sequenza sismica di Benevento (aprile-maggio 1990). Atti del 9 Convegno Nazionale GNGTS.

Iannaccone, G., Improta, L., Biella, G., Castellano, M., Deschamps, A., De Franco, R., Zollo, A., 1995. A study of local site effects in Benevento (Southern Italy) by the analysis of seismic records of explosions. Ann. Geophys. 38 (3–4).

Iannaccone, G., Improta, L., Capuano, P., Zollo, A., Biella, G., De Franco, R., Romeo, R., 1998. A P-wave velocity model of the upper crust of the Sannio region (Southern Apennines, Italy). Ann. Geophys. 41 (4).

Improta, L., Iannaccone, G., Capuano, P., Zollo, A., Scandone, P., 2000. Inferences on the upper crustal structure of Southern Apennines (Italy) from seismic refraction investigations and subsurface data. Tectonophysics 317 (3), 273–298.

Lin, G., Shearer, P., Hauksson, E., 2007. Applying a three-dimensional velocity model, waveform cross correlation, and cluster analysis to locate southern California seismicity from 1981 to 2005. J. Geophys. Res. 112 (B12309), 14. http://dx.doi.org/10.1029/2007JB004986.

Lomax, A., Virieux, J., Volant, P., Thierry, B.C., 2000. Probabilistic earthquake location in 3D and layered models: introduction of a Metropolis–Gibbs method and comparison with linear locations. In: Thurber, C.H., Rabinowitz, N. (Eds.), Advances in Seismic Event Location. Kluwer Academic, Amsterdam, pp. 101–134.

Madariaga, R., 1976. Dynamics of an expanding circular fault. Bull. Seismol. Soc. Am. 66 (3), 639–666.

Menardi Noguera, A., Rea, G., 2000. Deep structure of the Campanian–Lucanian Arc (Southern Apennine, Italy). Tectonophysics 324, 239–265.

Michele, M., Custódio, S., Emolo, A., 2014. Moment tensor resolution: case study of the Irpinia Seismic Network, Southern Italy. Bull. Seismol. Soc. Am. 104 (3), 1348–1357. http://dx.doi.org/10.1785/0120130177.

Milano, G., Di Giovambattista, R., Alessio, G., 1999. Earthquake swarms in the Southern Apennines Chain (Italy): the 1997 seismic sequence in the Sannio–Matese mountains. Tectonophysics 306, 57–58.

Milano, G., Ventura, G., Di Giovambattista, R., 2002. Seismic evidence of longitudinal extension in the Southern Apennines chain (Italy): the 1997–1998 Sannio–Matese seismic sequence. Geophys. Res. Lett. 29 (20), 65-1.

Milano, G., Di Giovambattista, R., Ventura, G., 2006. Seismicity and stress field in the Sannio–Matese area. Ann. Geophys. supplement to vol. 49 (1).

Montone, P., Mariucci, M.T., Pierdominici, S., 2012. The Italian present-day stress map. Geophys. J. Int. 189 (2), 705–716.

Mostardini, F., Merlini, S., 1986. Appennino centro meridionale Sezioni geologiche e proposta di modello strutturale. Mem. Soc. Geol. Ital. 35, 177–202.

Nicolai, C., Gambini, R., 2007. Structural architecture of the Adria platform-and-basin system. Boll. Soc. Geol. Ital. Volume speciale (7), 21–37.

Pantosti, D., Valensise, G., 1990. Faulting mechanism and complexity of the 23 November, 1980, Campania–Lucania earthquake inferred from surface observations. J. Geophys. Res. 95 (B10), 15,319–15,341. http://dx.doi.org/10.1029/JB095iB10p15319.

Patacca, E., Scandone, P., 2001. Late thrust propagation and sedimentary response in the thrust–belt–foredeep system of the Southern Apennines (Pliocene–Pleistocene). In: Vai, G.B., Martini, I.P. (Eds.), Anatomy of an Orogen: The Apennines and the Adjacent Mediterranean Basins. Kluwer Academic Publishers, pp. 401–440.

Patacca, E., Scandone, P., 2007. Geology of the Southern Apennines. Boll. Soc. Geol. Ital. Volume speciale (7), 75–119.

Pierdominici, S., Heidbach, O., 2012. Stress field of Italy—mean stress orientation at different depths and wave-length of the stress pattern. Tectonophysics 532, 301–311.

Pieri, P., Festa, V., Moretti, M., Tropeano, M., 1997. Quaternary tectonic activity of the Murge area (Apulian foreland-Southern Italy). Ann. Geophys. 40 (5).

Reasenberg, P., Oppenheimer, D., 1985. FPFIT, FPPLOT and FPPAGE: FORTRAN computer programs for calculating and displaying earthquake fault-plane solutions. Open File Report 85-739. United States Geological Survey, pp. 85–739.

Romano, M.A., de Nardis, R., Garbin, M., Peruzza, L., Priolo, E., Lavecchia, G., Romanelli, M., 2013a. Temporary seismic monitoring of the Sulmona area (Abruzzo, Italy): quality study of microearthquake locations. Nat. Hazards Earth Syst. Sci. 13, 2727–2744.

Romano, M.A., de Nardis, R., Lavecchia, G., Garbin, M., Peruzza, L., Priolo, E., Lavecchia, G., Romanelli, M., Ferrarini, F., 2013b. Preliminary analysis of the microearthquakes–faults association in the Sulmona basin (central Apennines, Italy). Rend. Online Soc. Geol. Ital. 29, 150–153.

Rovida, A., Camassi, R., Gasperini, P., Stucchi, M., 2011. CPTI11, the 2011 Version of the Parametric Catalogue of Italian Earthquakes. http://dx.doi.org/10.6092/INGV.IT-CPTI11 (Milano, Bologna, http://emidius.mi.ingv.it/CPTI).

Rubin, A.M., Gillard, D., Got, J.L., 1999. Streaks of microearthquakes along creeping faults. Nature 400 (6745), 635–641.

Saikia, C.K., 1994. Modified frequency–wavenumber algorithm for regional seismograms using Filon's quadrature: modelling of Lg waves in eastern North America. Geophys. J. Int. 118 (1), 142–158.

Scholz, C.H., 2002. The Mechanics of Earthquakes and Faulting. Cambridge University Press.

Scognamiglio, L., Tinti, E., Michelini, A., 2009. Real-time determination of seismic moment tensor for the Italian region. Bull. Seismol. Soc. Am. 99 (4), 2223–2242.

Scrocca, D., Carminati, E., Doglioni, C., 2005. Deep structure of the southern Apennines, Italy: thin-skinned or thick-skinned? Tectonics 24, TC3005. http://dx.doi.org/10.1029/2004TC001634.

Scrocca, D., Sciamanna, S., Di Luzio, E., Tozzi, M., Nicolai, C., Gambini, R., 2007. Structural setting along the CROP-04 deep seismic profile (Southern Apennines—Italy). Boll. Soc. Geol. Ital. Volume speciale (7), 283–296.

Shiner, P., Beccacini, A., Mazzoli, S., 2004. Thin-skinned versus thick-skinned structural models for Apulian carbonate reservoirs: constraints from the Val d'Agri Fields, S. Apennines, Italy. Mar. Pet. Geol. 21 (2004), 805–827.

Stabile, T.A., Satriano, C., Orefice, A., Festa, G., Zollo, A., 2012. Anatomy of a microearthquake sequence on an active normal fault. Sci. Rep. 2, 410. http://dx.doi.org/10.1038/srep00410.

Tondi, E., Piccardi, L., Cacon, S., Kontny, B., Cello, G., 2005. Structural and time constraints for dextral shear along the seismogenic Mattinata fault (Gargano, southern Italy). J. Geodyn. 40, 134–152. http://dx.doi.org/10.1016/j. jog.2005.07.003.

Turino, C., Scafidi, D., Eva, E., Solarino, S., 2009. Inferences on active faults at the Southern Alps–Liguria basin junction from accurate analysis of low energy seismicity. Tectonophysics 475, 470–479. http://dx.doi.org/10.1016/j.tecto.2009.06.007.

Valensise, G., Pantosti, D., 2001. The investigation of potential earthquake sources in peninsular Italy: a review. J. Seismol. 5 (3), 287–306.

Valensise, G., Pantosti, D., Basili, R., 2004. Seismology and tectonic setting of the 2002 Molise, Italy, earthquake. Earthquake Spectra 20, S23–S37. http://dx.doi.org/10.1193/1.1756136.

Vallée, M., 2004. Stabilizing the empirical Green function analysis: development of the projected Landweber method. Bull. Seismol. Soc. Am. 94, 394–409.

Vezzani, L., Festa, A., Ghisetti, F.C., 2010. Geology and tectonic evolution of the Central-Southern Apennines, Italy. Geol. Soc. Am. Spec. Pap. 469, 1–58.

Waldhauser, F., Ellsworth, W.L., 2000. A double-difference earthquake location algorithm: method and application to the northern Hayward Fault, California. Bull. Seismol. Soc. Am. 90, 1353–1368.

Weber, E., Convertito, V., Iannaccone, G., Zollo, A., Bobbio, A., Cantore, L., Corciulo, M., Di Crosta, M., Elia, L., Martino, C., Romeo, A., Satriano, C., 2007. An advanced seismic network in the Southern Apennines (Italy) for seismicity investigations and experimentation with earthquake early warning. Seismol. Res. Lett. 78 (6), 622–634. http://dx.doi.org/10.1785/gssrl.78.6.622.

Westaway, R., Jackson, J.A., 1987. The earthquake of 1980 November 23 in Campania–Basilicata (Southern Italy). Geophys. J. R. Astron. Soc. 90, 375–443. http://dx.doi.org/10.1111/j.1365-246X.1987.tb00733.x.

DISS Working Group, 2010. Database of Individual Seismogenic Sources (DISS). Version 3.1.1: A Compilation of Potential Sources for Earthquakes Larger Than M5.5 in Italy and Surrounding Areas: Available From the Istituto Nazionale di Geofisica e Vulcanologia (INGV) at http://diss.rm.ingv.it/dissNet/ (last accessed July 2014).

Zambonelli, E., de Nardis, R., Filippi, L., Nicoletti, M., Dolce, M., 2011. Performance of the Italian strong motion network during the 2009, L'Aquila seismic sequence (central Italy). Bull. Earthq. Eng. 9, 39–65.

Zollo, A., Orefice, A., Convertito, V., 2014. Source parameter scaling and radiation efficiency of microearthquakes along the Irpinia fault zone in southern Apennines, Italy. J. Geophys. Res. Solid Earth 119, 3256–3275. http://dx.doi.org/10.1002/2013JB010116.

Please cite this article as: Adinolfi, G.M., et al., The September 27, 2012, M_L 4.1, Benevento earthquake: A case of strike-slip faulting in Southern Apennines (Italy), Tectonophysics (2015), http://dx.doi.org/10.1016/j.tecto.2015.06.036